

# An Investigation of the Long and Short Ranges Interactions in BCC and FCC Spherical Metallic Nanocrystals

Esam H. Abdul Hafidh

Yanbu University College, Department of Physics  
Yanbu, Saudi Arabia  
essama@yuc.edu.sa

**Abstract-** *The contribution of the long and short range terms of the atom-atom interaction within nanocrystals has been investigated using three different models. Lennard-Jones, Mie-Type, and Mie-type combined with Axilrod-Teller potential energy functions have been used for the comparison between the short and long range terms. Physical importance of these models can be understood by studying the behaviour of long and short range terms of these potentials. In this paper a study on these terms for BCC and FCC nanocrystals has been carried out. The study was conducted by computer simulation and predicted size dependence of the ratio of the short range to the long range terms. Mie-type combined with Axilrod-Teller potential successfully describes the mutual variation of long and short range terms.*

**Keywords:** Short Range Interaction, Long Range Interaction, Potential Energy Function, Nanocrystals

© Copyright 2012 Authors - This is an Open Access article published under the Creative Commons Attribution License terms (<http://creativecommons.org/licenses/by/2.0>). Unrestricted use, distribution, and reproduction in any medium are permitted, provided the original work is properly cited.

## 1. Introduction

Several researchers have tried to simulate the nature of atom-atom interaction, the stability, lattice constant, cohesive energy, and melting phenomena of nanocrystals during the last decade. Models like the surface area difference [SAD] (Qi & Wang, 2002), the extended surface area difference [ESAD] (Qi et al., 2007a), the generalized surface area difference [GSAD] (Qi 2006a), the liquid drop model [LD] (Nanda et al., 2002), the latent heat model [LH] (Jiang et al., 2002a), the bond energy model [BE] (Qi et al. 2003), the extended bond energy model [EBE] (Qi et al. 2006b), the generalized bond

energy [GBE] (Qi et al. 2007b), the bond-order-length-strength model [BOLS] (Chang et al., 2002 ) were successful to predict the cohesive energy of nanocrystals. The melting temperature and the cohesive energy change linearly. Many researchers (Safai et al., 2007, Qi & Wang 2004a, Qi 2005, Jiang et al., 2000b, Zhang et al., 2000) successfully modelled and predicted the melting temperature of some nanomaterials. Other researchers, found quite a distinct structure properties between nanoparticles and nanostructured materials (Y. F. Zhu, et al., 2009). It was noted that some researchers used potential energy functions (PEF) that describe the atom-atom interaction in the bulk material for modelling the atom-atom interactions in the nanocrystals. It must be realized that the interaction within the nanocrystals is totally different from that in bulk material. Whereas, in bulk crystals, the atoms are affected by the electron sea field, they are affected in the nanocrystals by Van Der Waals interactions formed by dipoles. The dipoles are formed by the electron clouds along with atoms. This paper develops a test to check whether a PEF correctly describes the interaction within the nanocrystals or not.

There were two main approaches to model the atom-atom interactions in nanocrystals: (i) consider the two, three-body interactions (Qi et al., 2004b, Barakat et al., 2007, Barakat et al., 2009, El-Bayyari 1992a,b, Erkoc 1985, 1988, 1989a,b, 1990, 1992, 1997, 2000 Coles 1990) or (ii) consider the bulk and surface parameters (number of bonds, surface energy, melting entropy, etc.). The size dependence of the thermodynamic quantities of metallic particles was reported as early as 1909 (Jiang et al., 2002a).

Non-bonded interactions can be divided into two classes: short and long range interactions. The short range repulsive forces result from the overlapping of electron cloud. The models investigated in this paper comprise at least two inverse power terms. The ratios of the powers range between

“1” and “2”. One of the terms is attractive (negative potential energy) and the other is repulsive (positive potential energy). The attractive term is considered to be “long range” while the repulsive term is “short range”. The attractive term has been found to have less exponent power than the repulsive (Kittel 1995). Long range and short range terms have always been an interest for scientists involved in research related to molecular dynamics, molecular interactions, condensed matter, and nano-science.

In this paper models and methods of the calculation are explained in section 2. Following that the discussion of the findings and results are given in section 3 and concluding remarks are given in section 4.

## 2. Model and Method of Calculations

The method adopted in this study is based on the size dependent potential parameters (SDPP) method. The metallic nanocrystals are generated from ideal FCC and BCC crystal structures assuming a similar internal structure of the bulk. The method of counting particles in a given size is simple. One of the atoms is taken as the central one and the radii of the shells are integer multiples of the lattice parameter 'a'. The determination of the number of shells, the radius, the position of individual atoms and the total number of atoms in the nanocrystal can also easily be found.

The Three different models proposed by three research groups which successfully describe the size dependence of the cohesive energy of nanocrystals follow:

(i) Lennard-Jones model where atoms are assumed to interact via the potential: (Deltour et al. 1997)

$$U_{ij} = 4\epsilon \left[ \left( \frac{r_o}{r_{ij}} \right)^{12} - \left( \frac{r_o}{r_{ij}} \right)^6 \right]. \quad (1)$$

(ii) Mie-type model with the atom-atom interaction described via the potential: (Aydogdu & Sever, 2010)

$$U_{ij} = \frac{\epsilon}{m-k} \left[ k \left( \frac{r_o}{r_{ij}} \right)^m - m \left( \frac{r_o}{r_{ij}} \right)^k \right], \quad (2)$$

where  $r_{ij}$  denotes the distance between atoms  $i$  and  $j$ ,  $r_o$  denotes the equilibrium separation between the centers of any two atoms,  $\epsilon$  denotes the pair energy at  $r_o$ ,  $m$ , and  $k$  are adjustable parameters.

(iii) A Mie-type combined with Axilrod-Teller three body term as: (Axilrod & Teller, 1943)

$$U_{2,ij} = \epsilon \left[ \left( \frac{r_o}{r_{ij}} \right)^8 - 2 \left( \frac{r_o}{r_{ij}} \right)^4 \right], \quad (3)$$

$$U_{3,ijk} = \frac{z(1+3\cos\theta_i\cos\theta_j\cos\theta_k)}{(r_{ij}r_{jk}r_{ik})^3}, \quad (4)$$

where  $\theta_i$ ,  $\theta_j$ ,  $\theta_k$  and  $r_{ij}$ ,  $r_{jk}$ ,  $r_{ik}$  represents the angles and the sides of the triangle formed by the three atoms,  $i$ ,  $j$ , and  $k$  respectively. The parameter  $z$  is the intensity of the three body interaction.

The internal energy is given by the sum of the potential and the kinetic energies. At 0 K the total energy is given by the potential energy. It was found that the difference between the cohesive energies of bulk metals at 0 K and their melting temperatures are less than 5% (Kittel 1995). So, in this study, the calculations are conducted at 0 K and the total energy can be found by summing the potential over all the atoms in the nanocrystal as (for model (i)):

$$E_n = 2\epsilon \sum_{i=1}^n \sum_{j=1, j \neq i}^n \left[ \left( \frac{r_o}{r_{ij}} \right)^{12} - \left( \frac{r_o}{r_{ij}} \right)^6 \right], \quad (5)$$

which can be written as;

$$E_n = 2\epsilon \sum_{i=1}^n \sum_{j=1, j \neq i}^n \left[ \frac{\left( \frac{r_o}{d} \right)^{12} \left( \frac{d}{a} \right)^{12}}{\left( \frac{r_{ij}}{a} \right)^{12}} - \frac{\left( \frac{r_o}{d} \right)^6 \left( \frac{d}{a} \right)^6}{\left( \frac{r_{ij}}{a} \right)^6} \right] \quad (6)$$

Defining the geometrical factor 'g' as:

$$g = \frac{d}{a} \text{ and } r^* = \frac{r_o}{d} \quad (7 \& 8)$$

equation (6) reads

$$E_n = 2\epsilon \sum_{i=1}^n \sum_{j=1, j \neq i}^n \left[ \frac{g^{12} r^{*12}}{\left( \frac{r_{ij}}{a} \right)^{12}} - \frac{g^6 r^{*6}}{\left( \frac{r_{ij}}{a} \right)^6} \right] \quad (9)$$

'g' has definite values for each structure. It has the values of  $(\sqrt{3})/2$  for BCC and  $1/(\sqrt{2})$  for FCC structures.

$r_{ij}/a$  is the same for all elements of the same structure, so eq. (9) will describe fairly well the behaviour of all elements of a certain structure.

The binding energy per atom of a spherical metallic nanocrystal with cubic structure is:

$$E_a = \frac{E_n}{n\epsilon} = 2 \sum_{i=1}^n \sum_{j=1, j \neq i}^n \left[ \frac{g^{12} r^{*12}}{\left( \frac{r_{ij}}{a} \right)^{12}} - \frac{g^6 r^{*6}}{\left( \frac{r_{ij}}{a} \right)^6} \right] \quad (10)$$

$$E_a = 2A_{12} r^{*12} - 2A_6 r^{*6}, \quad (11)$$

where

$$A_{12} = \frac{1}{n} \sum_{i=1}^n \sum_{j=1, j \neq i}^n \frac{g^{12}}{\left(\frac{r_{ij}}{a}\right)^{12}} \quad (12)$$

And

$$A_6 = \frac{1}{n} \sum_{i=1}^n \sum_{j=1, j \neq i}^n \frac{g^6}{\left(\frac{r_{ij}}{a}\right)^6} \quad (13)$$

The stability condition for cubic crystals ( $\partial E_a / \partial V = 0$ ) at  $T=0$  K is imposed to obtain the minimum energy configuration. ( $\frac{\partial E_a}{\partial V} = 0$ ) which is equivalent to  $\partial E_a / \partial d = 0$ , since  $V$  and  $d$  are related via the relation  $V = N_o g d^3$ , where  $N_o$  is Avogadro's number. That means

$$2A_{12}r^{*12} - A_6r^{*6} = 0,$$

and

$$r^* = \left(\frac{A_6}{2A_{12}}\right)^{1/6} \quad (14)$$

the ratio of short range to long range terms is given by:

$$\Delta = \frac{A_{12}r^{*12}}{A_6r^{*6}} = \frac{1}{2}. \quad (15)$$

Similarly for model (ii), the total energy per atom can be written as:

$$E_a = 5A_6r^{*6} - 6A_5r^{*5} \quad (16)$$

The stability condition reveals that:

$$r^* = \frac{A_5}{A_6}, \quad (17)$$

for which the ratio  $\Delta$  is given by

$$\Delta = \frac{5A_6}{6A_5} r^* \quad (18)$$

The results in eqs. (15) and (18) can be generalized for two-body Mie-type potential to have:

$$\Delta = \frac{k}{m} \quad (19)$$

The total energy for the last model to be discussed in this paper is given by:

$$E_a = \frac{\epsilon}{2!} \sum_{i=1}^n \sum_{j=1, j \neq i}^n \left[ \left(\frac{r_o}{r_{ij}}\right)^8 - 2\left(\frac{r_o}{r_{ij}}\right)^4 \right] + \frac{z}{3!} \sum_{i,j,k, i \neq j \neq k}^n \frac{(1 + 3\cos\theta_i \cos\theta_j \cos\theta_k)}{(r_{ij}r_{jk}r_{ik})^3}, \quad (20)$$

which can be written as:

$$E_n = \frac{1}{2n} \sum_{i=1}^n \sum_{j=1, j \neq i}^n \left[ \frac{g^8 r^{*8}}{\left(\frac{r_{ij}}{a}\right)^8} - \frac{g^4 r^{*4}}{\left(\frac{r_{ij}}{a}\right)^4} \right] + \frac{z}{6\epsilon n} \sum_{i,j,k, i \neq j \neq k}^n \frac{(1 + 3\cos\theta_i \cos\theta_j \cos\theta_k)}{(r_{ij}r_{jk}r_{ik})^3} \quad (21)$$

with  $g$  and  $r^*$  defined as in eqs. (7) and (8).

Let

$$A_8 = \frac{1}{n} \sum_{i=1}^n \sum_{j=1, j \neq i}^n \frac{g^8}{\left(\frac{r_{ij}}{a}\right)^8}, A_4 = \frac{1}{n} \sum_{i=1}^n \sum_{j=1, j \neq i}^n \frac{g^4}{\left(\frac{r_{ij}}{a}\right)^4} \quad (22)$$

$$T_h = \frac{g^6}{6n} \sum_{i,j,k, i \neq j \neq k}^n \frac{(1 + 3\cos\theta_i \cos\theta_j \cos\theta_k)}{(r_{ij}r_{jk}r_{ik})^3}, Z^* = \frac{z}{\epsilon r_o^9} \quad (23)$$

Equation (21) can be written as

$$E_a = \frac{1}{2} A_8 r^{*8} - A_4 r^{*4} + z^* T_h r^{*9} \quad (24)$$

The stability equations reveal:

$$A_8 r^{*4} - A_4 + \frac{9}{4} z^* T_h r^{*5} = 0 \quad (25)$$

As the size of nanocrystal changes, the ratio  $r^*$  changes. The values of  $A_4$ ,  $A_5$ ,  $A_6$ ,  $A_8$ ,  $A_{12}$ , and  $T_h$  for FCC and BCC structures are given as a function of the number of atoms 'n' in the crystal in figures 1, 2, and 3 respectively. From these figures, it is apprehensible that the parameters  $A_i$  and  $T_h$  depend on the structure of the nanocrystal. In addition,  $A_i$  depends on the exponent of  $r_{ij}/a$ . As the exponent approaches  $\infty$ ,  $A_i$  approaches the number of nearest neighbours of a certain structure. The ratio  $r_{ij}/a$  represents the locations of the lattice points in space for the respective structure. Therefore, the summation can be easily found by summing

over all lattice points within the spherical shell of the nanocrystal.  $z^*$  is the intensity of the three-body term in the potential and can be found where FCC and BCC have a common minimum energy. The value was found by T, Barakat et al. (Barakat et al. 2009) to be 0.72. As such  $r^*$  can be found from equation (25) and its value depends on the nanocrystal size and structure as shown in figure 4.

For this model, the three-body term acts either as a short range, a long range or as a mixture of both (medium range). In general it ranges between 24-30% of the long range two-body term, so it does not affect the behaviour of  $\Delta$  in general, since it changes very slowly.

$$\Delta = \frac{\frac{1}{2}A_8 r^{*8}}{A_4 r^{*4}} = \frac{1}{2} \left( \frac{A_8}{A_4} \right) r^{*4} \quad (26)$$

The ratio  $\Delta$  as a function of  $n$  is shown in figure 5, where it shows size dependence for BCC and FCC, respectively. The long range term is dominant and the short range forms 23% to 17% of the long range for both FCC and BCC structures.

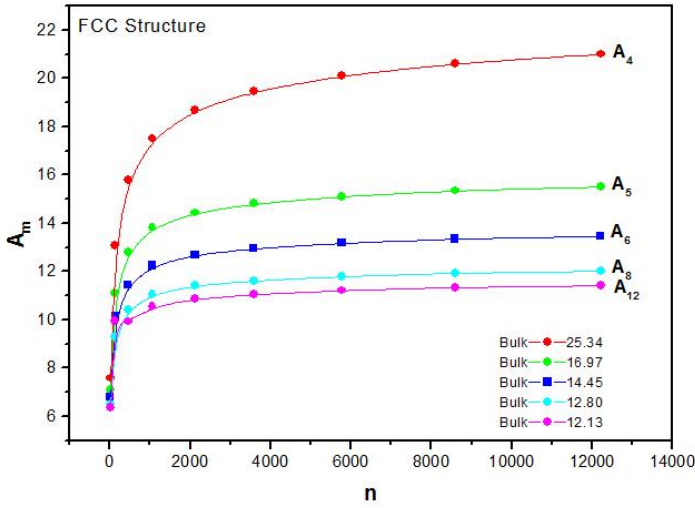


Fig. 1. The lattice sums  $A_4$ ,  $A_5$ ,  $A_6$ ,  $A_8$ , and  $A_{12}$  for FCC structure as a function of the number of atoms " $n$ ".

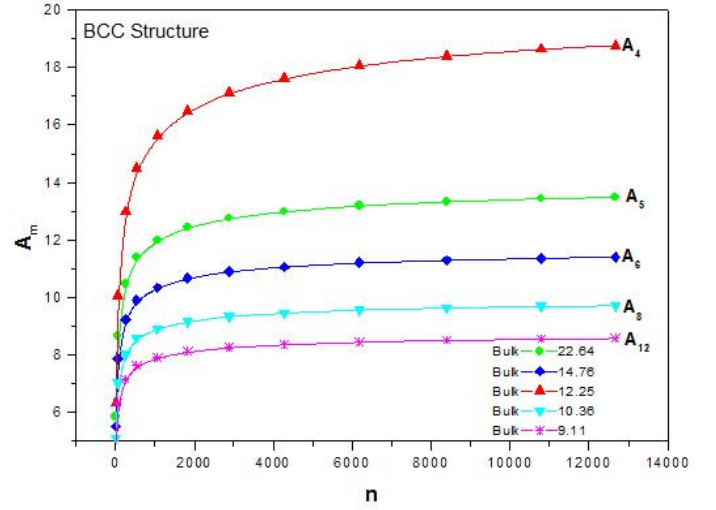


Fig. 2. The lattice sums  $A_4$ ,  $A_5$ ,  $A_6$ ,  $A_8$ , and  $A_{12}$  for BCC structure as a function of the number of atoms " $n$ ".

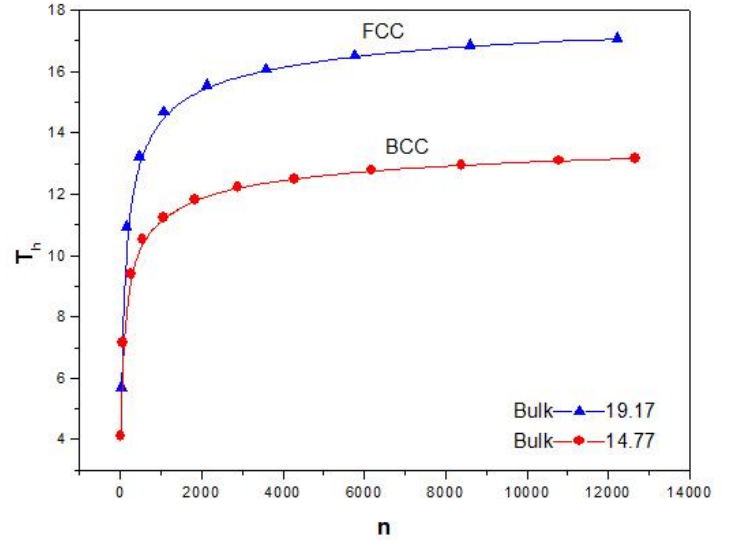


Fig. 3. The potential parameter  $T_h$  for FCC and BCC structures as a function of the number of atoms " $n$ ".

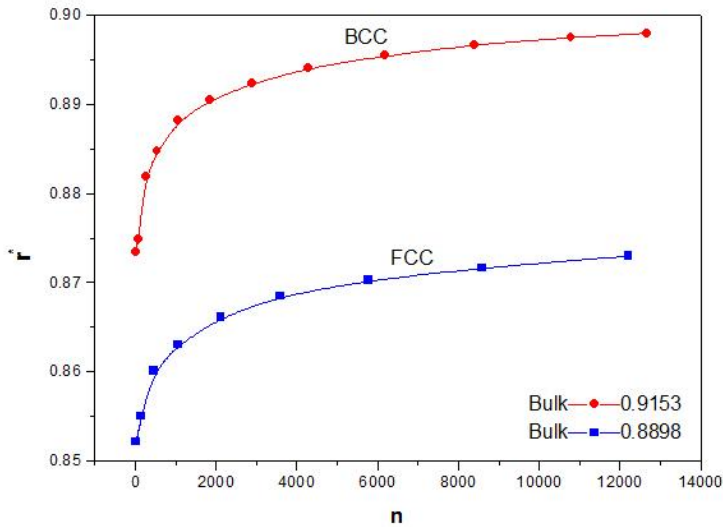


Fig. 4: The instantaneous dual change of  $r_o$  and  $d$  for BCC and FCC structures as a function of the number of atoms “n”.

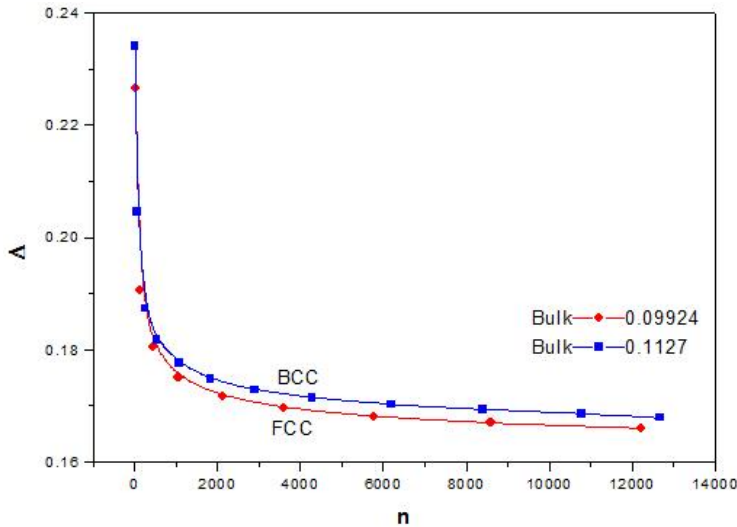


Fig. 5. The ratio of long and short range interaction factors for BCC and FCC structures as a function of the number of atoms “n”.

### 3. Discussion

The two models proposed by W. Qi et al. (Qi W. H. et al. 2004b) and T. Barakat et al. (Barakat T. et al. 2009) which include the Lennard-Jones (12,6) and Mie-type (6,5) respectively, reveal a constant ratio between the long and short range terms of the potential. For Lennard-Jones potential the long range term is twice that of the short range regardless of the structure and the size. For the Mie-Type (6,5),  $\Delta$  approaches unity, as if the short range and long range are equal. The effects of long range and short range overlap.

Figures 1, 2, and 3 show the size dependence of the lattice sums for FCC and BCC structures. It can be seen from these figures that these parameters increase rapidly as the

size of the nanocrystal increases and converge to their bulk values as  $n$  reaches 2000 atoms.

The ratio  $r^*$  represents the instantaneous dual change of  $r_o$  and  $d$ . It is given by  $r_o/d$  or equivalently by  $r_o/ag$ , where “a” is the lattice constant. Figure 4 show its size dependence as well as its quick convergence towards the bulk values for both FCC and BCC. This figure shows that  $r^*$  increases as the size increases. This means that the lattice constant “a” decreases as the size increases. It is quite interesting and unclear that “a” decreases as the size increases for nanoparticles, while the reverse is predicted for nanostructured materials.

The ratio of the short to the long range terms is shown in figure 5 for both FCC and BCC respectively.  $\Delta$  approaches 10% at the bulk. The short range term is crucial for small nanocrystals where it forms 23% of the long range term. It decreases rapidly and starts saturating at  $n$  greater than 2000 atoms.

### 4. Conclusion

Three models for the potential energy function have been used to investigate the test proposed in this paper. The first was the two-body Lennard-Jones, the second was the Mie-type with (m, k) as (6, 5) and the third is composed of a Mie-type with (m, k) as (8, 4) combined with Axilrod-Teller triple dipole terms. Different parameters and lattice sums of all the three PEF's were calculated where they showed size dependence and the correct convergence toward their bulk values. Models (i) and (ii) revealed a constant ratio of the short- to the long-range terms of the PEFs as 0.5 and 0.83 respectively. These results contradict the acceptable behaviour of the short and long range terms as one expects an increase in short range term when the atoms get closer and vice versa.

Model (iii) predicted to a high accuracy the experimental data for Mo and W. According to present work based on this model, the ratio of the short- to the long-range terms of the PEFs initially decreases rapidly with increasing the number of atoms in the nanocrystal reaching 170% of its bulk value at  $n = 2000$  atoms. On increasing the number of atoms, the  $\Delta$  exhibits a gradual decrease till the number of atoms in the nanocrystal exceeds 12000 for both FCC and BCC structures. The three-body part was fine tuned by the parameter  $z^*$  to give a stability condition at  $z^* = 0.72$  for both FCC and BCC structures. In conclusion, this work demonstrates the dependence of both the short- and long-range terms of the potential energy function of metallic nanocrystals on the range of the potential as well as the size and structure.

Model (iii) also in specific, describes correctly the behaviour of the ratio at the extremes values( i.e.  $n$  approaches to 0 and bulk) where the long range term gets smaller and larger respectively.

## References

- Axilrod, B. M., Teller, E. (1943). Interaction of the van der Waals Type Between Three Atom, *Journal of Chemical Physics* 11, 299.
- Aydogdu, O., Sever, R. (2010). Exact solution of the Dirac equation with the Mie-type potential under the pseudospin and spin symmetry limit, *Annals of Physics*, 35(20, 373-383.
- Barakat, T., Al-Dossary, O. M. (2007). and Alharbi A. A., The effect of Mie-type potential range on the cohesive energy of metallic nanoparticles, *International Journal of Nanoscience* 6, 461.
- Barakat, T., Al-Dossary, O. M., and Abdul-Hafidh, E. H. (2009). An investigation of the size-dependent cohesive energy and the structural stability of spherical metallic nanoparticles, *Journal of Physics B* 42.
- Benedek, G., Nardelli, G. F. (1967). Lattice Response Functions of Imperfect Crystals: Effects due to a Local Change of Mass and Short Range interaction, *Physical Review*, 155, 1004—1019.
- Coles, G. (Ed.) (1990). *The Chemical Physics Of Atomic and Molecular Clusters*, North-Holland, Amsterdam.
- Chang, Q. S., Wang, Y., Tay, B. K., Li, S., Huang, H., Zhang, Y. B. (2002). Correlation between the Melting Point of a Nanosolid and the Cohesive Energy of a Surface Atom, *Journal of Physical Chemistry B* 106, 10701.
- Deltour, P., Barrat, J. L., Jenson, P. (1997). Fast diffusion of a Lennard-Jones cluster on a crystalline surface, *Physical Review Letter*, 78, 4597.
- El-Bayyari, Z. (1992a). Phd Thesis, Middle East Technical University.
- El-Bayyari, Z., Erkoc S. (1992b). Molecular-Dynamics Computer Simulation of Aluminum Clusters (Al(n); n=3-55): Empirical Many-Body Potential Energy Function Calculation, *Physica Status Solidi (b)* 170, 103.
- Erkoc, S., (1985). *Doga Bilim Dergisi Seri A1*, Cilt 9, Sayi 3, 203.
- Erkoc, S., Katircioglu, S. (1988). Molecular Dynamics Simulation of Gold Microclusters, *Chemical Physics Letter*, 47, 476.
- Erkoc, S., Katircioglu S. (1989a). Molecular Dynamics Simulation of Aluminum Microclusters, *Physica Status Solidi(b)* 152, K37.
- Erkoc, S. (1989b). A New Empirical Many-Body Potential Energy Function: Application to microclusters, *Physica Status Solidi (b)* 152, 447.
- Erkoc, S. (1990a). Structural stability and energetics of F.C.C Metal microclusters, *Physica Status Solidi(b)* 161, 211.
- Erkoc, S. (1992). A New Class of Empirical Many-Body Potential Energy Function for Bulk and Cluster Properties: Application to fcc Metals, *Physica Status Solidi(b)* 171, 317.
- Erkoc, S. (1997). Empirical many-body potential energy functions used in computer simulations of condensed matter properties, *Physical Reports* 278, 79.
- Erkoc, S. (2000). Stability of Gold Clusters: Molecular-Dynamics Simulations, *Physica E* 8, 210
- Jiang, Q., Li, J. C., Chi, B. Q. (2002a). Size-dependent cohesive energy of nanocrystals, *Chemical Physics Letter* 366, 551.
- Jiang, Q., Zhang, Z., Li, J. C. (2000b). Melting thermodynamics of nanocrystals embedded in a matrix, *Acta Materialia* 48, 4791.
- Kittel, C. (1995). *Introduction to Solid State Physics*, 7th ed., Wiley, New York, p.65.
- Sattler, K. D. (2011). *Clusters and Fullerenes*, CRC Press, Taylor & Francis Group.
- Lucas, A. (1967). Collective Contributions to the Long-Range Dipolar Interaction in Rare-Gas Crystals, *Physica*, 35, 3.
- Nanda, K. K., Sahu, S. N., Behera, S. N. (2002). Liquid-drop model for the size-dependent melting of low-dimensional systems, *Physical Review A* 66, 013208.
- Qi, W. H., Wang, M. P. (2002). Size effect on the cohesive energy of nanoparticle, *Journal of Materials Science* 21, 1743.
- Qi, W. H., Wang, M. P. Xu, G. Y., (2003). The particle size dependence of cohesive energy of metallic nanoparticles, *Chemical Physics Letter* 372, 632.
- Qi, W. H., Wang, M. P., (2004a). Size and shape dependent melting temperature of metallic nanoparticles, *Materials Chemistry and Physics*, 88(2-3), 280-284.
- Qi, W. H., Wang, M. P, Zhou, M., Hu, W. Y. (2004b). Calculation of the cohesive energy of metallic nanoparticles by the Lennard-Jones potential, *Materials Letters* 58, 1745.
- Qi, W. H. (2005). Size effect on melting temperature of nanosolids, *Physica B* 368, 46.
- Qi, W. H. (2006a). Generalized Surface-Area-Difference model for cohesive energy of nanoparticles with different compositions, *J. Mater. Sci.* 41, 5679.
- Qi, W. H., Wang M. P, Zhou M., Shen X. Q., Zhang X. F. (2006b). Modeling cohesive energy and melting temperature of nanocrystals, *Journal of Physical Chemistry Of Solids* 67, 851.
- Qi, W. H., Wang M. P, Li Z., Hu W. Y. (2007a). Surface-Area-Difference Model for Melting Temperature of Metallic Nanocrystals Embedded in a Matrix, *Solid State Phenomena* 121, 1181.
- Qi, W. H. , Huang B. Y., Wang M. P, Li Z., Yu Z. M. (2007b). Generalized bond-energy model for cohesive energy of small metallic particles, *Physica Letter A* 370, 494.
- Rhee, M., Zbib, H. M., Hirth, J. P., Huang, H., de la Rubia, T. (1998). Models for long-/short-range interactions and cross slip in 3D dislocation simulation of BCC single crystals, *Modelling and Simulation in Materials Science and Engineering* 6, 467.
- Ruhwandl, R. W., Terentjev, E. M. (1997) Long-range forces and aggregation of colloid particles in a nematic liquid crystal, *Physical Review E* 55, 2958—2961.
- Safai, A., Shandiz, M. A., Sanjabi, S., Barber, Z. H. (2007). Modelling the size effect on the melting temperature of nanoparticles, nanowires and nanofilms, *Journal of Physics: Condensed Matter* 19, 216216.

- Sutton, A. P., Chen, J. (1990). Long-range Finnis--Sinclair potentials, *Philosophical Magazine Letters*, Volume 61, Issue 3.
- Tanaka, S., Scheraga, H. A. (1976) Medium- and Long-Range Interaction Parameters between Amino Acids for Predicting Three-Dimensional Structures of Proteins, *Macromolecules*, 9 (6), pp 945—950.
- Zhang, A., Li, J. C., Jiang, Q. (2000). Modelling for size-dependent and dimension-dependent melting of nanocrystals, *Journal of Physics D: Applied Physics* 33, 2653.
- Zhu, Y. F., Zheng, W. T., Jiang, Q. (2009) Modelling lattice expansion and cohesive energy of nanostructured materials. *Applied Physical Letter* 95, 083110.
- Zhu, Y. F., Lian, J. S., Jiang, Q. (2009) Modelling the melting point, Debye Temperature, Thermal Expansion Coefficient and Specific Heat of nanostructured materials. *Journal of Physical Chemistry C*. 133, 16896.